Achieving Low Overpotential Li-O_2 Battery Operations by Li_2O_2 Decomposition through One-electron Processes

Jin Xie[1], Qi Dong[1], Ian Madden[1], Xiahui Yao[1], Qingmei Cheng[1], Paul Dornath[2], Wei Fan[2], and Dunwei Wang[1,*]

[1] Department of Chemistry, Merkert Chemistry Center, Boston College, 2609 Beacon St., Chestnut Hill, MA, 02467 USA

[2] Department of Chemical Engineering, University of Massachusetts, 686 North Pleasant St., Amherst, MA, 01003 USA

[*] Email: dunwei.wang@bc.edu; Tel: +1-617-552-3121; Fax: +1-617-552-2705

Table of Contents in Supplementary Information

Experimental details:

Materials Preparation:

Carbon cathode synthesis: 3DOm carbon was prepared following a previously reported recipe[1]. Briefly, the process involved 7 key steps: (1) a silica colloidal crystal template composed of highly monodisperse silica nanoparticles (SNPs; d~35 nm) was impregnated with furfuryl alcohol and oxalic acid (precursors) with a weight ratio of 200:1; (2) the system was allowed to polymerize at 70 °C for 48 hours; (3) it was then cured at 200 °C in N_2 for 3 h; (4) the sample was carbonized at 900 °C for 2 h; (5) SNPs were removed in 6 M KOH solution at 150 °C for 48 h; (6) the resulting carbon material was thoroughly rinsed with deionized water at 70 °C until the resulting solution was neutral; (7) the final product was dry at 70 °C for 24 h. Prior to construction of Li-O_2 test cells, the as-prepared 3DOm carbon was annealed in H_2 (5 sccm, standard cubic centimeter per minute) Ar (95 sccm) at 950 °C for 6 h (pressure 5 torr).

Electrochemical characterizations:

Carbon and polytetrafluoroethylene (PTFE) were mixed in isopropyl alcohol (IPA) with a weight ratio of 95:5. The mixture was sonicated for 60 min at room temperature and then deposited onto a compressed Ni foam (original thickness 1.6 mm; MTI Corp.). The resulting electrode was further dried in the antechamber attached to the glove box (MBraun) under active vacuum at 100 °C for 12 h. The loading density of carbon on electrodes was between 0.20 to 0.25 mg/cm^2.

$PYR_{14}TFSI$ (99.9%) was purchased from Solvionic. The ionic liquid was further dried in the antechamber attached to the glove box under active vacuum at 80°C for 48 h. $LiClO_4$ (99.99%, Battery grade, Sigma-Aldrich) was baked at 80 °C in the antechamber under active vacuum at for

48 h and then mixed with $PYR_{14}TFSI$ to produce a 0.1 M electrolyte solution. All chemicals were transferred into glovebox from antechamber without exposing to atmosphere to avoid H_2O contamination. 0.1 M $LiClO_4$ in dimethoxyethane (DME) was used as purchased from Novolyte (BASF) with water level <10 ppm.

Customized Swagelok^{TM} type cells were assembled in the glove box (H_2O and O_2 levels < 0.1 ppm, MBraun) using Li metal (380μm in thickness, Sigma-Aldrich) as the anode, Celgard 2400 film as the separator, and 200μL electrolyte. The cells were characterized using a potentiostat (VMP3, Bio-Logic).

Iodometric titration:

For titration experiments, Swagelok^{TM} cells were dissembled in an O_2-tolerated Ar-filled glove box (H_2O level < 0.1 ppm, MBraun) immediately after discharging. For each individual cell, both working electrode and electrolyte were collected in glass vials for titration. 1.0 mL DME was used to wash the cell and the resulting solution was also collected for titration. The sealed vials were then transferred out of the glove box and 0.5 mL H_2O was injected immediately. The reaction mixture of 0.2 mL $PYR_{14}TFSI$, 0.5 mL H_2O and 1.0 mL DME formed a homogenous monophasic solution to ensure the completeness of reaction between Li_2O_2 and H_2O. The reaction mixture was then sonicated for 2 min to fully decompose Li_2O_2 deposited inside the mesopores of a-3DOm carbon. After removing Ni foam, 2 mL H_2O and 0.1 mL 6 M HCl were successively added to the homogenous mixture to separate the ionic liquid phase and the aqueous phase. Due to the surface hydrophobic nature of a-3DOm carbon, majority of the product was extracted in the ionic liquid phase, and the light absorption by carbon did not interfere with the

detection of titration end point. The ionic liquid phase was further washed by 1.0 mL H_2O three times to fully extract remaining H_2O_2. The rinsing solution was combined with the separated aqueous phase as titrate. Prior to the titration, 0.5 mL 2% KI solution and 50 μL Mo catalyst solution[2] were added. The reaction mixture was then titrated using a pre-calibrated $Na_2S_2O_3$ solution.

Control experiments were conducted to ensure the accuracy of phase separation method and the influence of carbon cathode composition. Commercially available Li_2O_2 powder (90%, Sigma-Aldrich) was applied for comparison. The purity of the commercial Li_2O_2 powder was determined as 85% by standard iodometric titration. By adding DME with ionic liquid so as to emulate our phase separation method, the purity as detected was 2% less (83% yield), which accounts for the H_2O_2 loss during phase separation, solution transfer, rinsing and the minuscule solubility of H_2O_2 in ionic liquid. The effect of carbon cathode composition was further investigated by introducing three types of carbon materials into the homogeneous titrate prior to the phase separation. A-3DOm carbon, as-prepared 3DOm carbon and Vulcan XC72 carbon could all be extracted into the ionic liquid phase after phase separation, therefore their influence on titration end point detection can be evaluated. Using the procedure described above, the purities of commercial Li_2O_2 powder with a-3DOm carbon, original 3DOm carbon and Vulcan carbon were determined as 80%, 72% and 79%, respectively. The decrease of the purity from 82% can be attributed to the different reactivity and absorption between carbon and H_2O_2.[3]

Superoxide detection using nitrotetrazolium blue chloride:

Nitrotetrazolium blue chloride dye (2,2'-bis(4-Nitrophenyl)-5,5'-diphenyl-3,3'-(3,3'-dimethoxy-4,4'-diphenylene) ditetrazolium chloride, ~98%, TLC, Sigma Aldrich) was applied to selectively detect superoxide species and differentiate it from peroxide[4]. If superoxide species exists, the dye will go through a color change from light yellow to dark blue. Anhydrous DME was used to disperse the dye. Cells containing a-3DOm carbon cathode in $PYR_{14}TFSI$ electrolyte and in DME electrolyte were prepared and discharged to the same capacity. Commercial Li_2O_2 preloaded on a-3DOm carbon cathode with $PYR_{14}TFSI$ electrolyte in an electrochemical cell case was also prepared as a control. Dye/DME solution was immediately injected into the coin cell negative case after cell disassembly. The Celgard separator with originally white color was taken out for photography and comparison. The procedure was carried out in the Ar-filled glovebox.

X-ray photoelectron spectroscopy:

Surface analysis was carried out using a K-Alpha XPS (Thermo Scientific). Customized Swagelok™ type cells[5] were first transferred into the Ar-filled glove box (H_2O level < 0.1 ppm, MBraun) and then disassembled. Cathode samples were then rinsed with pure anhydrous DME (Sigma-Aldrich) for three times to remove residual salts and/or ionic liquids. An airtight sample holder was used to transfer samples. Samples were then mounted on the stage with a short exposure to the ambient air (typically <5 min) before vacuuming the load lock. XPS data was fitted using XPS Peak 4.1 software.

Online Gas-Chromatography Mass Spectrometry:

The oxygen and carbon dioxide calibration curves were generated by manually injecting air (0.5 μL, 1 μL and 2 μL) at 298 K into the GCMS (Shimadzu QP2010 Ultra, with Carboxen 1010 PLOT column at 50°C) injection port, and the gas peak area was fitted into a linear relationship against gas volume with R^2 higher than 0.99. For the *in situ* gas evolution detection, previously discharged Swagelok™ type cell with a-3DOm carbon cathode and $PYR_{14}TFSI$ electrolyte was connected to the GCMS sampling loop (500 μL in volume) and a ultrahigh purity He carrier gas delivery line (10 sccm flow rate). In order to enhance the signal-to-noise ratios, a higher recharge rate and capacity were applied on a larger loading of a-3DOm carbon or Vulcan XC 72 carbon. The total discharge and recharge capacity was limited to 0.1 mAh for data acquisition and consistency with previous testing conditions. Before the recharge process, ultrahigh purity He gas was flowed through Swagelok™ type cell and sampling loop overnight to purge the system and evacuate residual gases. The system was allowed to rest for 1 h after the GCMS detector was turned on to stabilize the MS signal for a flat baseline. After the recharge was completed, the gaseous products were sampled for 2 h for the MS signals to reach a stable baseline level again. This step is important because it helps compensate for system errors induced by slow diffusion within the cell and in the gas lines. The area change of the MS signal during recharge was recorded for gas evolution and Faraday efficiency calculations.

NMR:

^1H NMR was performed on a 600 MHz spectrometer. Deuterated $CDCl_3$ (99.8%) was purchased from Cambridge Isotope Labs. All NMR chemical shifts were reported in ppm relative to residual solvent.

Figure S1: stability tests of ionic liquid based electrolyte

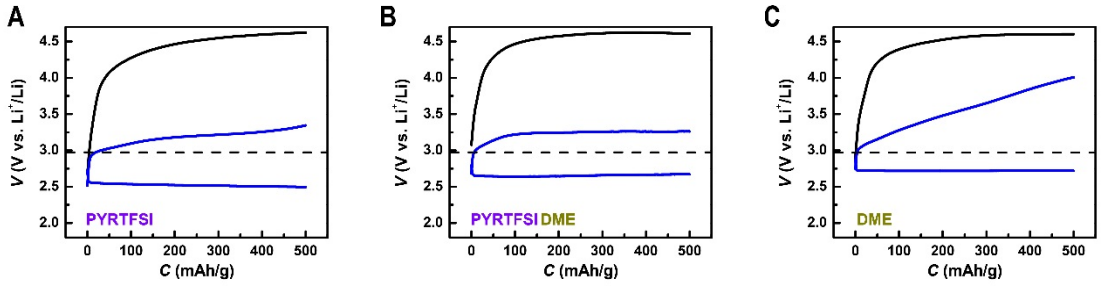

Figure S1: Stability tests of pure and mixed electrolytes in oxygen. (A) 0.1 M $LiClO_4$ in $PYR_{14}TFSI$ electrolyte; (B) 0.1 M $LiClO_4$ in 50% $PYR_{14}TFSI$ and 50% DME mixed electrolyte; (C) 0.1 M $LiClO_4$ in DME electrolyte.

In the electrolyte stability tests, we applied a charge current of 100 mA/g (the same rate as those in Figure 1 and Figure S5) to the electrodes directly without first discharging in O_2. Compared to typical discharge/charge profiles (in blue) acquired under the same testing condition (100 mA/g in O_2), the direct recharge potential (in black) quickly reached a plateau close to 4.6V vs. Li^+/Li, which corresponds to the decomposition potential of the electrolytes.

Figure S2: detailed titration results

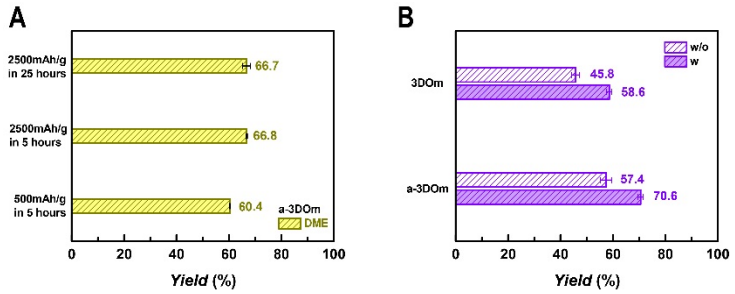

Figure S2: Product detection. (A) Iodometric titration results of a-3DOm carbon samples discharged under different discharging conditions in DME. Filled bars are the yield with the electrolyte also titrated. (B) Iodometric titration results of pristine 3DOm carbon samples and a-3DOm carbon samples discharged in $PYR_{14}TFSI$. Filled bars are the yield with the electrolyte also titrated and open bars are the yield only from the cathode support.

In Figure S2A, we found the titration yields were sensitive to discharge conditions. For cells discharged to deeper discharge depth, the acquired yields were higher.

In Figure S2B, we compared the titration yields between a-3DOm carbon and as-prepared 3DOm carbon. We found that annealing was important as it helped to remove surface functional groups. Discharge yields were improved using a-3DOm carbon.

Figure S3: detection of superoxide radical by nitrotetrazolium blue chloride

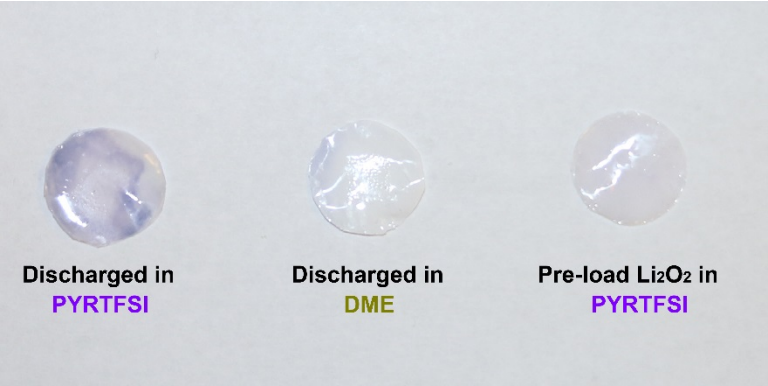

Figure S3: Detection of superoxide radical by nitrotetrazolium blue chloride. (A). Discharged in $PYR_{14}TFSI$; (B) Discharged in DME; (C) Pre-load commercial Li_2O_2 in $PYR_{14}TFSI$.

In Figure S3, superoxide radicals were detected by nitrotetrazolium blue chloride. No obvious color change was observed in $PYR_{14}TFSI$ electrolyte pre-loaded with commercial Li_2O_2 powders, or in discharged cell with DME electrolyte.

Figure S4: detailed NMR results

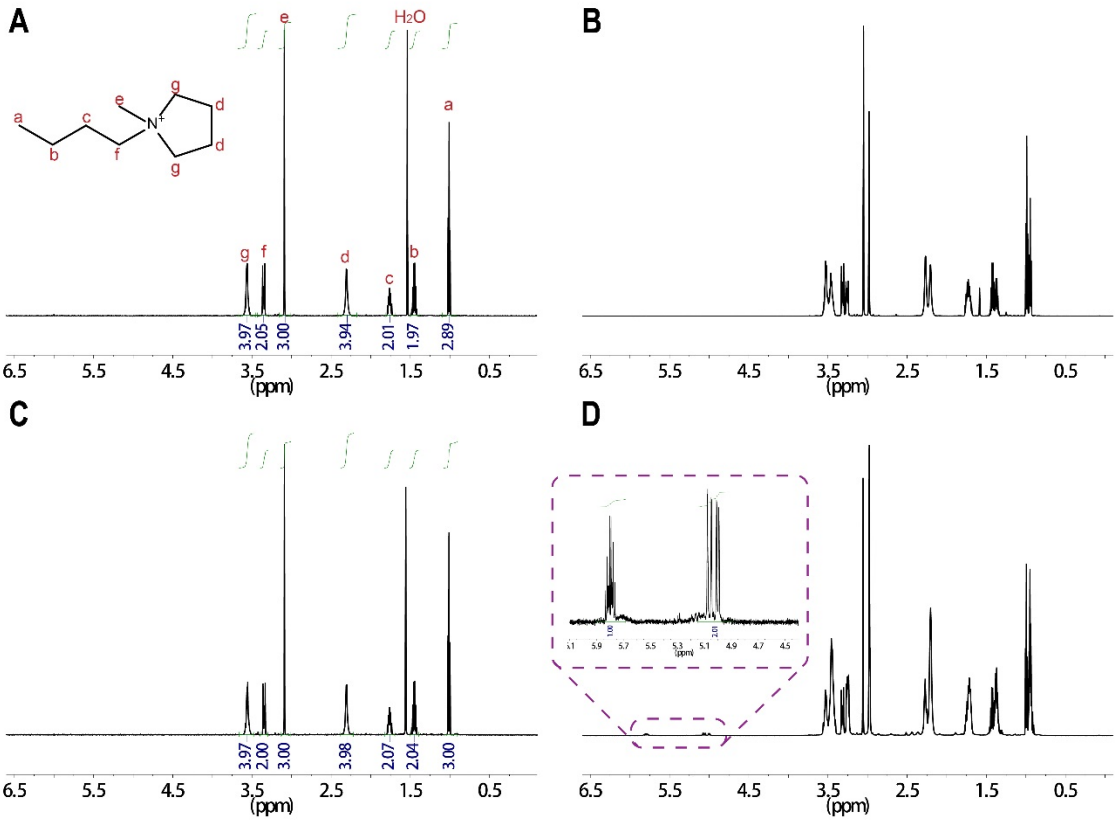

Figure S4: NMR characterization of pristine $PYR_{14}TFSI$ electrolyte (0.1 M $LiClO_4$) at low concentration (A) and high concentration (B); NMR characterization of cycled $PYR_{14}TFSI$ electrolyte (0.1 M $LiClO_4$) at low concentration (C) and high concentration (D).

The purity of $PYR_{14}TFSI$ electrolyte was investigated by NMR characterizations. The NMR spectrum of the pristine $PYR_{14}TFSI$ electrolyte (0.1 M $LiClO_4$ in $PYR_{14}TFSI$) was shown in Figure S4A. All proton peaks can be assigned to $PYR_{14}TFSI$ with the exception of the one close to 1.6 ppm, which is due to H_2O contamination in $CDCl_3$ used as the NMR solvent.

In Figure S4B, every peak (expect that for H_2O) split into two when a relatively high concentration (100 times more than the one tested in Figure S4A) of $PYR_{14}TFSI$ electrolyte was dissolved in $CDCl_3$. The reason, as reported by Hesse-Ertelt et al.,[6] is due to the strong ion-ion interaction so that two types of PYR^+ coexisted. One is solvated by $CDCl_3$ and the other formed ion pairs with $TFSI^-$. However, as we can see from both Figure S4A and S4B, no impurities peaks have been detected, supporting that the $PYR_{14}TFSI$ electrolyte was of high purity.

By comparison, $PYR_{14}TFSI$ electrolyte (0.1 M $LiClO_4$ in $PYR_{14}TFSI$) was analyzed by NMR after 16 repeated cycles. When a low concentration of cycled $PYR_{14}TFSI$ electrolyte was tested, a clean spectrum without peak splitting nor byproduct peaks were generated in Figure S4C.

When $PYR_{14}TFSI$ electrolyte concentration increased 100 times in $CDCl_3$, peak splitting was observed in Figure S4D. In addition, weak byproduct peaks were also found (inset in Figure S4D). Although the absolute concentration of byproduct is small, it shows characteristics of alkene byproducts with peak area ratio of 1:2. We propose such product were $PYR_{14}TFSI$ decomposition byproduct through a Hoffmann elimination process.

Figure S5: long term stability test with various electrolyte compositions

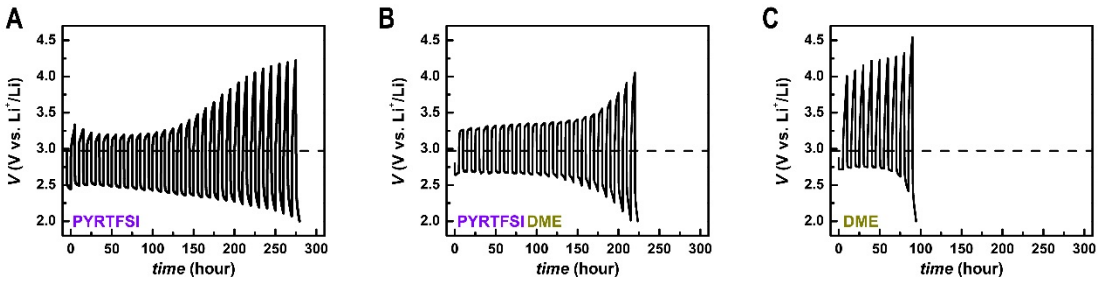

Figure S5: Long term stability of a-3DOm in various electrolytes. (A) 0.1 M $LiClO_4$ in $PYR_{14}TFSI$ electrolyte; (B) 0.1 M $LiClO_4$ in 50% $PYR_{14}TFSI$ and 50% DME mixed electrolyte; (C) 0.1 M $LiClO_4$ in DME electrolyte. The dotted horizontal line marks the thermodynamic equilibrium potential of 2.96V vs. Li^+/Li. Discharge/charge rate is 100mA/g_{carbon}.

Although the decomposition of $PYR_{14}TFSI$ is inevitable as shown in Figure S4, it is slightly more stable than DME as the discharge yield in $PYR_{14}TFSI$ is higher than in DME according to the titration results (Figure 3 in the main text). For long term stability test, we also found that cells using $PYR_{14}TFSI$ as electrolyte last longer than ones using DME electrolyte and $PYR_{14}TFSI$/DME mixed electrolyte.

Figure S6: cycle performance of Vulcan XC72 carbon

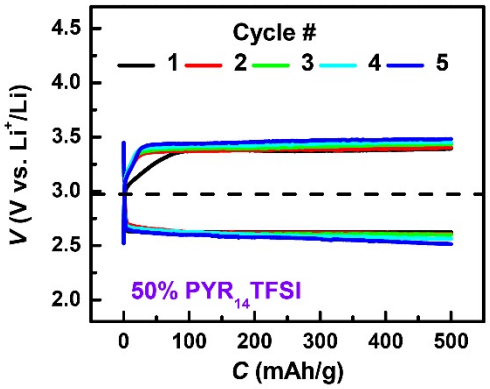

Figure S6: Discharge/recharge behaviors of Vulcan XC72 carbon in 50% $PYR_{14}TFSI$ (0.1M $LiClO_4$) and 50% DME (0.1M $LiClO_4$) electrolytes during the first five cycles.

The result indicates discharge/recharge overpotentials characteristic is not unique to a-3DOm carbon. Compare with Figure 1C (0.28V for discharge and 0.30V for recharge), both the average discharge overpotential (0.35V) and average recharge overpotential (0.44V) during the first five cycles were slightly higher in Figure S6 when Vulcan carbon was utilized, presumably due to the smaller surface area of Vulcan carbon compared to a-3DOm.

Figure S7: XPS characterization

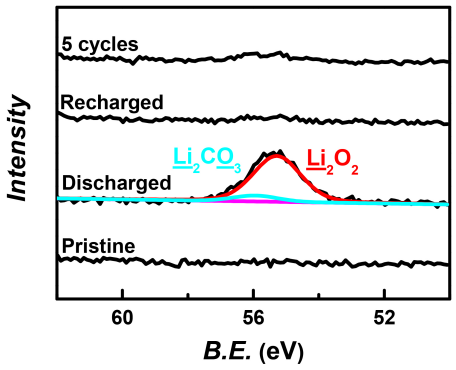

Figure S7: Li 1s X-ray photoelectron spectra of a-3DOm carbon cathode support after various experimental operations in 100% $PYR_{14}TFSI$ electrolyte (0.1M $LiClO_4$).

In agreement with Figure 4A, distinct Li peak corresponding to Li_2O_2 existed in discharged samples. This result, combined with NMR characterization, suggests the by-products are formed mainly in the solution phase, in contrast with the dominance of solid by-products formation in DME electrolyte.

References:

(1) Fan, W.; Snyder, M. A.; Kumar, S.; Lee, P. S.; Yoo, W. C.; McCormick, A. V.; Penn, R. L.; Stein, A.; Tsapatsis, M. *Nature Mater.* **2008,** *7,* 984-991.

(2) McCloskey, B. D.; Valery, A.; Luntz, A. C.; Gowda, S. R.; Wallraff, G. M.; Garcia, J. M.; Mori, T.; Krupp, L. E. *J Phys Chem Lett* **2013,** *4,* 2989-2993.

(3) Adams, B. D.; Black, R.; Radtke, C.; Williams, Z.; Mehdi, B. L.; Browning, N. D.; Nazar, L. F. *Acs Nano* **2014,** *8,* 12483-12493.

(4) Laoire, C. O.; Mukerjee, S.; Abraham, K. M.; Plichta, E. J.; Hendrickson, M. A. *J Phys Chem C* **2009,** *113,* 20127-20134.

(5) Xie, J.; Yao, X.; Cheng, Q.; Madden, I. P.; Dornath, P.; Chang, C.-C.; Fan, W.; Wang, D. *Angew. Chem. Int. Ed.* **2015,** *127,* 4373-4377.

(6) Hesse-Ertelt, S.; Heinze, T.; Kosan, B.; Schwtkal, K.; Meister, F. *Macromol. Symp.* **2010,** *294-II,* 75-89.